# Near Field Targets Localization Using Bistatic MIMO System with Symmetric Arrays

Parth Raj Singh
IETR
Polytech Nantes
France
Email: parth-raj.singh@etu.univ-nantes.fr

Yide Wang
IETR
Polytech Nantes
France
Email: yide.wang@univ-nantes.fr

Pascal Chargé
IETR
Polytech Nantes
France
Email: pascal.charge@univ-nantes.fr

***Abstract*—In this paper, we propose a subspace based method to localize multiple targets in the near field region of a bistatic MIMO system with symmetric uniform linear arrays (ULAs). The proposed method uses the symmetry in the transmitting and receiving arrays to estimate the angle of departure (AOD) and angle of arrival (AOA) of each target by using 1D rank reduction estimator (RARE) based method. For each estimated AOA, the range from the center of the transmitting array to the corresponding target is estimated by using 1D multiple signal classification (MUSIC). Finally, the receiver side range of each target is estimated by using the other three estimated location parameters in 2D MUSIC technique which also automatically pairs the location parameters.**

## I. Introduction

Directly or indirectly, the applications like radar, sonar, communication, etc. use the sources localization which makes it an important field of research. In the literature, there exist many passive sources localization methods [1]–[4]. However, to localize the objects which do not emit their own radiation, we need an active approach in which the objects are illuminated by one or more emitters. In this direction, MIMO system has received a lot of attention because it uses multiple transmitters emitting orthogonal signals that provide more degrees of freedom to improve the parameter identifiability and angular resolution [5], [6]. There exist many multiple targets localization techniques using a MIMO system. However, the majority of them are dedicated to far field targets in comparison to near field targets [7]–[11].

Near field targets cannot be handled like far field targets because the emitted or intercepted waves can no longer be considered as planar in the Fresnel region. Therefore, Fresnel approximation is usually made in the near field region, in which, the spherical wavefront is approximated as quadratic surface wavefront to simplify the signal model [1]–[4]. There are many near field sources localization methods in the literature, but only few directly deal with MIMO system [11]. In this paper, we propose a method to localize near field targets using bistatic MIMO system consisting of symmetric ULAs. The proposed method can be considered as an extension of the method in [3] to deal with the bistatic MIMO system. [3] uses two subarrays, however, the division of the array into two subarrays is unnecessary. Thus, in the proposed method, we use the whole array and its permuted version.

This work was supported by a grant from the 19th Fonds Unique Interministeriel (FUI) project, labeled as FUI-19 SLASH+ project (Solution de Localisation indoor Adaptée aux Services Hospitaliers).

This paper is organized as follows. Section II provides the signal model formulated for $P$ point targets in the near field region of a bistatic MIMO system with symmetric transmitting and receiving ULAs. Section III describes the proposed method to estimate the location parameters of targets viz. AOD and AOA, distances between the targets and the center of the transmitting array, and between the targets and the center of the receiving array. Section V shows the performance of the proposed method in terms of the estimation error of the location parameters.

*Notations*

$\odot$, $\otimes$, and $\boxdot$ respectively denote the Hadamard-Schur, Kronecker, and Khatri-Rao products. $\mathcal{E}\{\bullet\}$ is the expectation. $[\bullet]^*$, $[\bullet]^T$, and $[\bullet]^H$ respectively represent the conjugate, transpose, and Hermitian transpose of a matrix. $\mathbb{R}$ and $\mathbb{C}$ are the sets of all real and complex numbers respectively. $\mathfrak{Re}\{\bullet\}$ returns the real part of a complex number. $[\bullet]^{-1}$ and $\det\{\bullet\}$ respectively denote the inverse and determinant of a square matrix. $\boldsymbol{I}_N$ signifies an identity matrix of dimension $N \times N$. $\boldsymbol{J}_N$ denotes the permutation matrix of dimension $N \times N$ with ones along its main antidiagonal and zeros elsewhere. $\mathbf{1}_{M\times N}$ is the matrix of ones of dimension $M \times N$.

## II. Signal model

Consider a narrowband bistatic MIMO system with symmetric ULAs containing $\breve{M} = 2M + 1$ transmitting and $\breve{N} = 2N + 1$ receiving omnidirectional antennas. Let $d_e$ and $d_r$ be the distances between the consecutive antennas in the transmitting and receiving arrays respectively. Additionally, in the considered MIMO system, we assume that the signals emitted by all the transmitting antennas are temporally orthogonal, with same bandwidth and same carrier frequency. $P$ near field targets reflect the signals emitted by the omnidirectional transmitting antennas. Finally, the receiving array intercepts the reflections from these $P$ targets. At the receiving end, matched filters separate the orthogonal transmitted signals for each receiving antenna. In case of bistatic MIMO system, the

ISBN 978-0-9928626-7-1 © EURASIP 2017

received matched filtered signal data at time $t$, $\boldsymbol{y}(t)$, is usually modeled as [7]–[10]

$$\boldsymbol{y}(t) = \boldsymbol{C}\boldsymbol{s}(t) + \boldsymbol{n}(t) \tag{1}$$

where $\boldsymbol{s}(t) \in \mathbb{C}^{P\times 1}$, with zero mean and bounded variance, contains mutually independent random complex reflection coefficients of the $P$ near field targets which follow Swerling model II [12]. $\boldsymbol{n}(t)$ is the noise vector with spatially and temporally white complex Gaussian components with zero mean and variance $\sigma^2$. $\boldsymbol{C} = \boldsymbol{A} \boxdot \boldsymbol{B} \in \mathbb{C}^{\breve{M}\breve{N}\times P}$ where

$$\boldsymbol{A} = [\boldsymbol{a}(\rho_{e_1}, \theta_{e_1}),\, \boldsymbol{a}(\rho_{e_2}, \theta_{e_2}),\, \cdots,\, \boldsymbol{a}(\rho_{e_P}, \theta_{e_P})] \tag{2}$$

and

$$\boldsymbol{B} = [\boldsymbol{b}(\rho_{r_1}, \theta_{r_1}),\, \boldsymbol{b}(\rho_{r_2}, \theta_{r_2}),\, \cdots,\, \boldsymbol{b}(\rho_{r_P}, \theta_{r_P})] \tag{3}$$

are the directional matrices of $P$ targets associated with the transmitting and receiving arrays respectively. $\boldsymbol{A} \in \mathbb{C}^{\breve{M}\times P}$ and $\boldsymbol{B} \in \mathbb{C}^{\breve{N}\times P}$. $\rho_{e_p}$ and $\rho_{r_p}$ are the distances to the $p$th target from the centers of the transmitting and receiving arrays respectively where $p \in \{1, 2, \cdots, P\}$. $\theta_{e_p}$ is the AOD belonging to the $p$th target measured at the center of the transmitting array with respect to the axis of the array and $\theta_{r_p}$ is the AOA of the $p$th target measured at the center of the receiving array with respect to its axis. $\theta_{e_p}$ and $\theta_{r_p}$ may vary from $0°$ to $180°$. $\boldsymbol{a}(\rho_{e_p}, \theta_{e_p})$ and $\boldsymbol{b}(\rho_{r_p}, \theta_{r_p})$ are respectively the directional vectors of departure and arrival associated with the $p$th target.

The component of $\boldsymbol{a}(\rho_{e_p}, \theta_{e_p})$ corresponding to index $m \in \{-M, \cdots, -1, 0, 1, \cdots, M\}$ can be written as [1]

$$a(m,p) = \exp(-j\,2\,\pi\,\delta(m,p)/\lambda) \tag{4}$$

where $\lambda$ is the wavelength of the carrier wave and

$$\delta(m,p) = \sqrt{\rho_{e_p}^2 + m^2\,d_e^2 - 2\,m\,d_e\,\rho_{e_p}\cos(\theta_{e_p})} - \rho_{e_p} \tag{5}$$

is the difference between the distance traveled by the spherical wavefront of the signal emitted by the transmitting antenna with index $m$ to reach the $p$th target and the distance traveled by the wavefront of the signal emitted by the middle transmitting antenna with index 0 to reach the same $p$th target.

The near field (Fresnel) region of the transmitting ULA is a finite space around it bounded by the following lower and upper limits of $\rho_{e_p}$ [3], [13]:

$$r_{L_e} = 0.62((2\,M\,d_e)^3/\lambda)^{1/2} \tag{6}$$

and

$$r_{U_e} = 2(2\,M\,d_e)^2/\lambda. \tag{7}$$

In the near field region of the transmitting array, $\delta(m,p)$ is approximated by using the second order Taylor expansion of (5) [1]–[4], [11]

$$\delta(m,p) \approx -m\,\omega_{e_p} + m^2\,\phi_{e_p} \tag{8}$$

with $\omega_{e_p} = d_e\,\cos(\theta_{e_p})$ and $\phi_{e_p} = d_e^2\,\sin^2(\theta_{e_p})/(2\,\rho_{e_p})$. In terms of the approximated wavefront (8), the directional vector of departure can be expressed as

$$\boldsymbol{a}(\rho_{e_p}, \theta_{e_p}) = \begin{bmatrix} \exp(-j\,2\,\pi\,(M\,\omega_{e_p} + M^2\,\phi_{e_p})/\lambda) \\ \vdots \\ 1 \\ \vdots \\ \exp(-j\,2\,\pi\,(-m\,\omega_{e_p} + m^2\,\phi_{e_p})/\lambda) \\ \vdots \\ \exp(-j\,2\,\pi\,(-M\,\omega_{e_p} + M^2\,\phi_{e_p})/\lambda) \end{bmatrix}. \tag{9}$$

The Fresnel approximation made above, for the transmitting ULA, is also applicable to the receiving ULA. Using the similar approach, we can express the $p$th directional vector of arrival as

$$\boldsymbol{b}(\rho_{r_p}, \theta_{r_p}) = \begin{bmatrix} \exp(-j\,2\,\pi\,(N\,\omega_{r_p} + N^2\,\phi_{r_p})/\lambda) \\ \vdots \\ 1 \\ \vdots \\ \exp(-j\,2\,\pi\,(-n\,\omega_{r_p} + n^2\,\phi_{r_p})/\lambda) \\ \vdots \\ \exp(-j\,2\,\pi\,(-N\,\omega_{r_p} + N^2\,\phi_{r_p})/\lambda) \end{bmatrix} \tag{10}$$

where $\omega_{r_p} = d_r\,\cos(\theta_{r_p})$, $\phi_{r_p} = d_r^2\,\sin^2(\theta_{r_p})/(2\,\rho_{r_p})$, and $n \in \{-N, \cdots, -1, 0, 1, \cdots, N\}$. Like before, the lower and upper bounds of $\rho_{r_p}$ in the near field region of the receiving array can be calculated as $r_{L_r} = 0.62((2\,N\,d_r)^3/\lambda)^{1/2}$ and $r_{U_r} = 2(2\,N\,d_r)^2/\lambda$ respectively [3], [13].

## III. Proposed Method

The symmetry in the transmitting ULA allows us to write the following relation

$$\breve{\boldsymbol{J}}\,\boldsymbol{C} = (\boldsymbol{D_e} \boxdot \boldsymbol{1}_{\breve{N}\times P}) \odot \boldsymbol{C} \tag{11}$$

where $\breve{\boldsymbol{J}} = \boldsymbol{J}_{\breve{M}} \otimes \boldsymbol{I}_{\breve{N}}$ and $\boldsymbol{D_e} = [\boldsymbol{d_e}(\theta_{e_1}),\, \boldsymbol{d_e}(\theta_{e_2}),\, \cdots,\, \boldsymbol{d_e}(\theta_{e_P})]$ with

$$\boldsymbol{d_e}(\theta_{e_p}) = \begin{bmatrix} \exp(j\,4\,\pi\,M\,\omega_{e_p}/\lambda) \\ \vdots \\ 1 \\ \vdots \\ \exp(-j\,4\,\pi\,m\,\omega_{e_p}/\lambda) \\ \vdots \\ \exp(-j\,4\,\pi\,M\,\omega_{e_p}/\lambda) \end{bmatrix} \tag{12}$$

whose $m$th component is given by $a(-m,p)\,a^*(m,p)$. As mentioned in [3], $d_e \leq \lambda/4$ is a necessary condition to avoid the phase ambiguity in the elements of $\boldsymbol{D_e}$.

The covariance matrix of $\boldsymbol{y}(t)$ is given by

$$\begin{aligned}\boldsymbol{R} &= \mathcal{E}\{\boldsymbol{y}(t)\,\boldsymbol{y}^H(t)\} \in \mathbb{C}^{\breve{M}\breve{N}\times\breve{M}\breve{N}} \\ &= \boldsymbol{C}\,\boldsymbol{R_s}\,\boldsymbol{C}^H + \sigma^2\boldsymbol{I}_{\breve{M}\breve{N}}\end{aligned} \tag{13}$$

ISBN 978-0-9928626-7-1 

where $\boldsymbol{R_s} = \mathcal{E}\{\boldsymbol{s}(t)\,\boldsymbol{s}^H(t)\}$ is the reflection coefficient covariance matrix. The eigendecomposition of $\boldsymbol{R}$ can be written as

$$\boldsymbol{R} = \boldsymbol{U_s}\,\boldsymbol{\Lambda_s}\,\boldsymbol{U_s}^H + \sigma^2 \boldsymbol{U_n}\boldsymbol{U_n}^H \tag{14}$$

where the diagonal elements of $\boldsymbol{\Lambda_s} \in \mathbb{R}^{P\times P}$ are the $P$ largest eigenvalues and the columns of $\boldsymbol{U_s} \in \mathbb{C}^{\breve{M}\breve{N}\times P}$ are their corresponding eigenvectors spanning the signal subspace. We assume that the number of targets, $P$, is known. The columns of $\boldsymbol{U_n} \in \mathbb{C}^{\breve{M}\breve{N}\times(\breve{M}\breve{N}-P)}$ span the noise subspace. From (13) and (14), we can write

$$\boldsymbol{C}\,\boldsymbol{T} = \boldsymbol{U_s} \tag{15}$$

with $\boldsymbol{T} \in \mathbb{C}^{P\times P}$ being an invertible square matrix.

For an arbitrary angle $\theta$, we can write

$$\begin{aligned}\boldsymbol{F_e}(\theta) &= \breve{\boldsymbol{J}}\,\boldsymbol{U_s} - [\boldsymbol{d_e}(\theta)\otimes \boldsymbol{1}_{\breve{N}\times P}]\odot \boldsymbol{U_s} &(16)\\ &= \breve{\boldsymbol{J}}\,\boldsymbol{C}\,\boldsymbol{T} - [\boldsymbol{d_e}(\theta)\otimes \boldsymbol{1}_{\breve{N}\times P}]\odot \boldsymbol{C}\,\boldsymbol{T}\\ &= (\boldsymbol{D_e}\boxdot \boldsymbol{1}_{\breve{N}\times P})\odot \boldsymbol{C}\,\boldsymbol{T}\\ &\quad - [\boldsymbol{d_e}(\theta)\otimes \boldsymbol{1}_{\breve{N}\times P}]\odot \boldsymbol{C}\,\boldsymbol{T}\\ &= \big([\boldsymbol{d_e}(\theta_{e_1}) - \boldsymbol{d_e}(\theta),\, \boldsymbol{d_e}(\theta_{e_2}) - \boldsymbol{d_e}(\theta),\, \cdots,\\ &\qquad \boldsymbol{d_e}(\theta_{e_P}) - \boldsymbol{d_e}(\theta)]\boxdot \boldsymbol{1}_{\breve{N}\times P}\big)\odot \boldsymbol{U_s} &(17)\end{aligned}$$

from (11) and (15) (see [3] and [14]). At $\theta = \theta_{e_p}$, all the components of the $p$th column of $\boldsymbol{F_e}(\theta)$ become zero and $\boldsymbol{F_e}(\theta)$ becomes rank deficient. Thus, we can use the following spectrum function to estimate AODs [3], [14]

$$S_e(\theta) = \frac{1}{\det\{\boldsymbol{F_e}^H(\theta)\,\boldsymbol{F_e}(\theta)\}}. \tag{18}$$

The estimated AODs (say $\hat{\theta}_{e_p}$) of $P$ targets correspond to the $P$ highest peaks of $S_e(\theta)$ when $\theta$ is varied from 0° to 180°.

The subspace spanned by the directional vector of departure is orthogonal to the noise subspace, therefore, the estimated range corresponding to $\hat{\theta}_{e_p}$ can be given by

$$\hat{\rho}_{e_p} = \underset{r_{L_e}\le\rho\le r_{U_e}}{\arg\max}\ \frac{1}{\det\{\boldsymbol{G}^H(\rho)\,\boldsymbol{G}(\rho)\}} \tag{19}$$

where $\boldsymbol{G}(\rho) = \boldsymbol{U_n}^H[\boldsymbol{a}(\rho,\,\hat{\theta}_{e_p})\otimes \boldsymbol{I}_{\breve{N}}] \in \mathbb{C}^{(\breve{M}\breve{N}-P)\times\breve{N}}$. In (19), when $\breve{M}\breve{N} - P \ge \breve{N}$ and $\rho \ne \rho_{e_p}$, $\boldsymbol{G}(\rho)$ has full rank and $\det\{\boldsymbol{G}^H(\rho)\,\boldsymbol{G}(\rho)\}$ is not zero. At $\rho = \rho_{e_p}$, $\det\{\boldsymbol{G}^H(\rho)\,\boldsymbol{G}(\rho)\}$ tends towards zero due to the orthogonality between the noise subspace and the subspace spanned by the directional vector of departure corresponding to the $p$th target.

Like the transmitting array, the receiving array is also a symmetric ULA. Therefore, we can write

$$\breve{\boldsymbol{I}}\,\boldsymbol{C} = (\boldsymbol{1}_{\breve{M}\times P}\boxdot \boldsymbol{D_r})\odot \boldsymbol{C} \tag{20}$$

where $\breve{\boldsymbol{I}} = \boldsymbol{I}_{\breve{M}}\otimes \boldsymbol{J}_{\breve{N}}$ and $\boldsymbol{D_r} = [\boldsymbol{d_r}(\theta_{r_1}),\, \boldsymbol{d_r}(\theta_{r_2}),\, \cdots,\, \boldsymbol{d_r}(\theta_{r_P})]$ with

$$\boldsymbol{d_r}(\theta_{r_p}) = \begin{bmatrix}\exp(j\,4\,\pi\,N\,\omega_{r_p}/\lambda)\\ \vdots\\ 1\\ \vdots\\ \exp(-j\,4\,\pi\,n\,\omega_{r_p}/\lambda)\\ \vdots\\ \exp(-j\,4\,\pi\,N\,\omega_{r_p}/\lambda)\end{bmatrix}. \tag{21}$$

$d_r \le \lambda/4$ is a necessary condition to avoid the phase ambiguity in the elements of $\boldsymbol{D_r}$ [3].

Like before, the AOAs can be estimated by using the following spectrum function

$$S_r(\theta) = \frac{1}{\det\{\boldsymbol{F_r}^H(\theta)\,\boldsymbol{F_r}(\theta)\}}. \tag{22}$$

where

$$\begin{aligned}\boldsymbol{F_r}(\theta) &= \breve{\boldsymbol{I}}\,\boldsymbol{U_s} - [\boldsymbol{1}_{\breve{M}\times P}\otimes \boldsymbol{d_r}(\theta)]\odot \boldsymbol{U_s} &(23)\\ &= \big(\boldsymbol{1}_{\breve{M}\times P}\boxdot [\boldsymbol{d_r}(\theta_{r_1}) - \boldsymbol{d_r}(\theta),\, \cdots,\\ &\qquad \boldsymbol{d_r}(\theta_{r_P}) - \boldsymbol{d_r}(\theta)]\big)\odot \boldsymbol{U_s} &(24)\end{aligned}$$

can be obtained from (15) and (20). The estimated AOAs (say $\hat{\theta}_{r_p}$) of $P$ targets correspond to the $P$ highest peaks of $S_r(\theta)$ when $\theta$ is varied from 0° to 180°. However, the AOAs are not paired.

Finally, to get the estimation of the receiver side range of the $p$th target, we use 2D MUSIC as

$$(\hat{\rho}_{r_p},\,\hat{\theta}_{r_p}) = \underset{\substack{r_{L_r}\le\rho\le r_{U_r}\\ \theta\in\{\hat{\theta}_{r_1},\cdots,\hat{\theta}_{r_P}\}}}{\arg\max}\ \frac{1}{\boldsymbol{b}^H(\rho,\,\theta)\,\boldsymbol{Q}\,\boldsymbol{b}(\rho,\,\theta)} \tag{25}$$

where $\boldsymbol{Q} = [\boldsymbol{a}(\hat{\rho}_{e_p},\,\hat{\theta}_{e_p})\otimes \boldsymbol{I}_{\breve{N}}]^H\,\boldsymbol{U_n}\,\boldsymbol{U_n}^H\,[\boldsymbol{a}(\hat{\rho}_{e_p},\,\hat{\theta}_{e_p})\otimes \boldsymbol{I}_{\breve{N}}]$. Here, $\theta$ is chosen from the set of unpaired AOAs which reduces the computational cost. 2D MUSIC automatically pairs the transmitting and receiving sides location parameters for each target.

Initially, all the $P$ AODs and AOAs are estimated in one 1D search each. And then, the ranges belonging to transmitting and receiving arrays of each target are estimated separately by handling one target at a time. Therefore, all the location parameters are automatically paired. Because of the spectral search based methods, the proposed method is slower than the method in [11]. Additionally, both methods use eigen decomposition, however, the proposed method has computational complexity of $\mathcal{O}(P\,\breve{M}^3\,\breve{N}^3)$ and method in [11] has complexity of $\mathcal{O}(\breve{N}^3)$. The large computation complexity of the proposed method is paid off by the maximum number of targets it can locate. The proposed method can locate $\breve{N}(\breve{M}-1)$ targets whereas the method in [11] can locate only $\breve{N}$ targets.

ISBN 978-0-9928626-7-1 © EURASIP 2017

## IV. Cramér-Rao lower bound

Cramér-Rao lower bound (CRLB) for the ranges and AOA of multiple near field sources has already been derived in [2] from [15]. Here, we directly use their closed form expression by making some minor modifications to adapt the four location parameters of each target due to the use of a bistatic MIMO system. The submatrix of the inverse of the Fischer information matrix corresponding to the desired parameters (i.e. the location parameters of $P$ targets) can be expressed as [2]

$$\mathbf{CRB}(\boldsymbol{\eta}) = \frac{\sigma^2}{2\,L}\left[\Re\mathfrak{e}\left\{\left(\mathring{\boldsymbol{D}}^H\,\boldsymbol{\Pi}_{\boldsymbol{C}}^{\perp}\,\mathring{\boldsymbol{D}}\right)\right.\right. \odot \left.\left.\left[\mathbf{1}_{4\times4}\otimes\left(\boldsymbol{R}_{\boldsymbol{s}}\,\boldsymbol{C}^H\,\boldsymbol{R}^{-1}\,\boldsymbol{C}\,\boldsymbol{R}_{\boldsymbol{s}}\right)^T\right]\right\}\right]^{-1} \quad (26)$$

where $\mathbf{CRB}(\boldsymbol{\eta}) \in \mathbb{R}^{4P\times4P}$, $\boldsymbol{\eta} = [\rho_{e_1}, \cdots, \rho_{e_P}, \theta_{e_1}, \cdots, \theta_{e_P}, \rho_{r_1}, \cdots, \rho_{r_P}, \theta_{r_1}, \cdots, \theta_{r_P}]^T$ is the vector of the desired location parameters of $P$ targets, $L$ is the number of data samples, $\boldsymbol{\Pi}_{\boldsymbol{C}}^{\perp} = \boldsymbol{I}_{\breve{M}\breve{N}} - \boldsymbol{C}\,(\boldsymbol{C}^H\,\boldsymbol{C})^{-1}\,\boldsymbol{C}^H$, and

$$\mathring{\boldsymbol{D}} = [\partial\boldsymbol{c}_1/\partial\rho_{e_1}, \cdots, \partial\boldsymbol{c}_P/\partial\rho_{e_P}, \partial\boldsymbol{c}_1/\partial\theta_{e_1}, \cdots \partial\boldsymbol{c}_P/\partial\theta_{e_P}, \partial\boldsymbol{c}_1/\partial\rho_{r_1}, \cdots, \partial\boldsymbol{c}_P/\partial\rho_{r_P}, \partial\boldsymbol{c}_1/\partial\theta_{r_1}, \cdots, \partial\boldsymbol{c}_P/\partial\theta_{r_P}] \quad (27)$$

with $\boldsymbol{c}_p = \boldsymbol{a}(\rho_{e_p}, \theta_{e_p}) \otimes \boldsymbol{b}(\rho_{r_p}, \theta_{r_p})$. The main diagonal of (26) contains lower bounds of all the location parameters in terms of variance for all the targets.

## V. Simulation results

As an example, we consider a bistatic MIMO system with $\breve{M} = 9$ $(M = 4)$ transmitting and $\breve{N} = 11$ $(N = 5)$ receiving antennas. Each ULA is symmetric with $d_e = d_r = \lambda/4$. In Fig. 1, Fig. 2, Fig. 3, and Fig. 4, we compare the RMSE in the location parameters (range associated with the transmitting array, AOD, range associated with the receiving array, and AOA respectively ) of two targets estimated by the proposed method and the method in [11] with respect to SNR. The SNR is varied from 0 dB to 30 dB with an interval of 5 dB. The location parameters $(\rho_{e_p}, \theta_{e_p}, \rho_{r_p}, \theta_{r_p})$ of the two targets are $(1.8\lambda, 40.5°, 2.8\lambda, 130.5°)$ and $(3\lambda, 120.5°, 4\lambda, 70.5°)$. $L = 1000$ samples and $K = 1000$ Monte Carlo trials are used to compute the RMSE from the following equation

$$\epsilon\,(\eta_p) = \sqrt{\frac{1}{K}\sum_{k=1}^{K}\left(\hat{\eta}_p(k) - \eta_p\right)^2} \quad (28)$$

where $\eta_p \in \{\rho_{e_p}, \theta_{e_p}, \rho_{r_p}, \theta_{r_p}\}$ and $\hat{\eta}_p(k) \in \{\hat{\rho}_{e_p}(k), \hat{\theta}_{e_p}(k), \hat{\rho}_{r_p}(k), \hat{\theta}_{r_p}(k)\}$ is the estimated value in the $k$th trial. The CRLBs of the location parameters are calculated from (26). Let $\mathrm{CRB}(\eta_p)$ be the CRLB of the $\eta_p$ parameter belonging to the $p$th target in terms of standard deviation.

From the figures, we can observe that the proposed method has better performance in terms of RMSE than that of the method in [11]. The primary reason of the poor performance of the method in [11] is that it does not exploit all the available information.

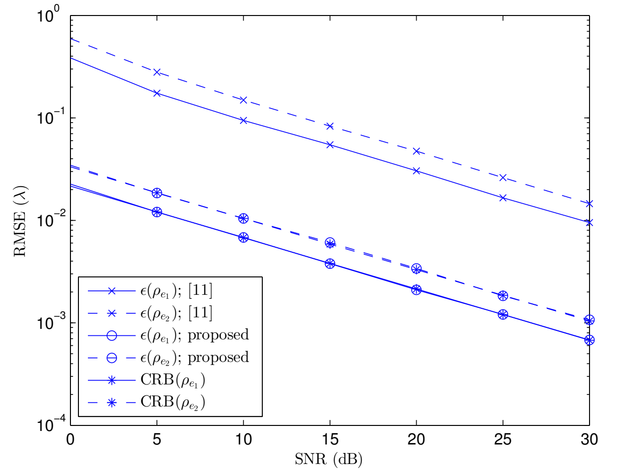


Fig. 1. RMSE in range associated with the transmitting array estimated by the method in [11] and the proposed method versus SNR.

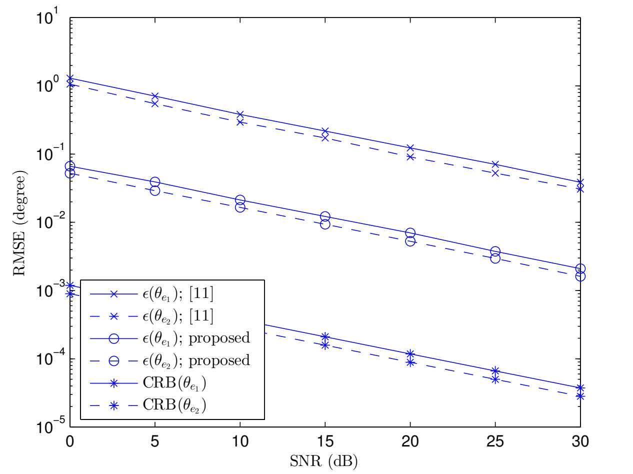


Fig. 2. RMSE in AOD estimated by the method in [11] and the proposed method versus SNR.

## VI. Conclusion

In this paper, we have proposed an extension of the method [3] to localize near field targets using a bistatic MIMO system consisting of symmetric transmitting and receiving ULAs. Compared to the existing method in [11], the proposed method has better performance because we exploit all the information. Along with it, the proposed method automatically pairs all the four location parameters. [11] uses submatrices of the covariance matrix, therefore, the maximum number of localizable targets is limited by the number of receiving antennas. For the proposed method, the maximum number of localizable targets is given by $\breve{N}(\breve{M} - 1)$.

As a future work, the performance of the proposed method can be investigated by applying the advanced covariance estimators [16]–[19] and by using real radar data in the presence of multipath effects [20].

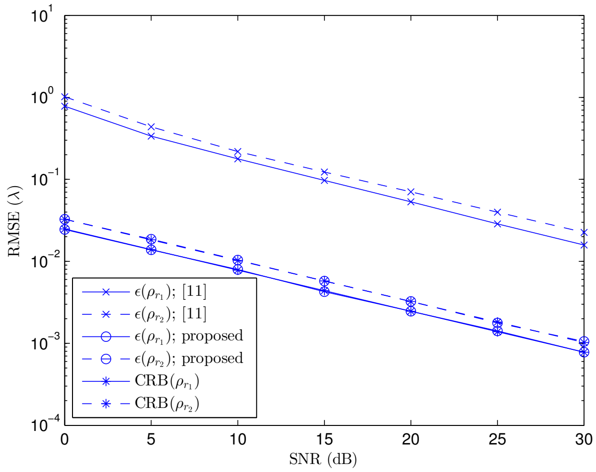


Fig. 3. RMSE in range associated with the receiving array estimated by the method in [11] and the proposed method versus SNR.

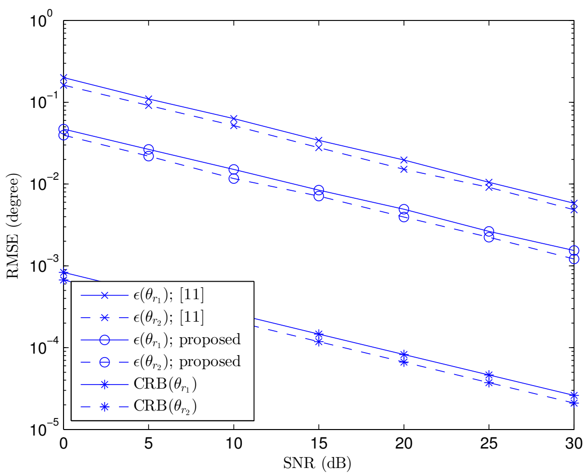


Fig. 4. RMSE in AOA estimated by the method in [11] and the proposed method versus SNR.

## References


[1] A. L. Swindlehurst and T. Kailath, "Passive direction-of-arrival and range estimation for near-field sources," in *Fourth Annual ASSP Workshop on Spectrum Estimation and Modeling*, Minneapolis, Minnesota, August 1988, pp. 123–128.

[2] E. Grosicki, K. Abed-Meraim, and Y. Hua, "A weighted linear prediction method for near-field source localization," *IEEE Trans. Signal Process.*, vol. 53, no. 10, pp. 3651–3660, 2005.

[3] W. Zhi and M. Y.-W. Chia, "Near-field source localization via symmetric subarrays," *IEEE Signal Process. Lett.*, vol. 14, no. 6, pp. 409–412, June 2007.

[4] L. Jianzhong, Y. Wang, and W. Gang, "Signal reconstruction for near-field source localisation," *IET Signal Processing*, vol. 9, no. 3, pp. 201–205, 2015.

[5] J. Li and P. Stoica, "MIMO radar with colocated antennas," *IEEE Signal Process. Mag.*, vol. 24, no. 5, pp. 106–114, September 2007.

[6] A. M. Haimovich, R. S. Blum, and L. J. Cimini, "MIMO radar with widely separated antennas," *IEEE Signal Process. Mag.*, vol. 25, no. 1, pp. 116–129, 2008.

[7] H. Yan, J. Li, and G. Liao, "Multitarget identification and localization using bistatic MIMO radar systems," *EURASIP Journal on Advances in Signal Processing*, vol. 2008, no. 1, pp. 1–8, 2007.

[8] D. Nion and N. D. Sidiropoulos, "A PARAFAC-based technique for detection and localization of multiple targets in a MIMO radar system," in *IEEE International Conference on Acoustics, Speech and Signal Processing (ICASSP)*, Taipei, Taiwan, April 2009, pp. 2077–2080.

[9] M. L. Bencheikh, Y. Wang, and H. He, "Polynomial root finding technique for joint DOA DOD estimation in bistatic MIMO radar," *Signal Processing*, vol. 90, no. 9, pp. 2723–2730, 2010.

[10] ——, "A subspace-based technique for joint DOA-DOD estimation in bistatic MIMO radar," in *11-th International Radar Symposium*, Vilnius, Lithuania, June 2010, pp. 1–4.

[11] E. Zhou, H. Jiang, and H. Qi, "4-D parameter estimation in bistatic MIMO radar for near-field target localization," in *International Wireless Symposium (IWS)*. Shenzhen, China: IEEE, March 2015, pp. 1–4.

[12] P. Swerling, "Probability of detection for fluctuating targets," *IRE Transactions on Information Theory*, vol. 6, no. 2, pp. 269–308, April 1960.

[13] Y. Begriche, M. Thameri, and K. Abed-Meraim, "Exact conditional and unconditional Cramér–Rao bounds for near field localization," *Digital Signal Processing*, vol. 31, pp. 45–58, April 2014.

[14] F. Gao and A. B. Gershman, "A generalized ESPRIT approach to direction-of-arrival estimation," *IEEE Signal Process. Lett.*, vol. 12, no. 3, pp. 254–257, March 2005.

[15] P. Stoica, E. G. Larsson, and A. B. Gershman, "The stochastic CRB for array processing: A textbook derivation," *IEEE Signal Process. Lett.*, vol. 8, no. 5, pp. 148–150, May 2001.

[16] A. De Maio, "Maximum likelihood estimation of structured persymmetric covariance matrices," *Signal processing*, vol. 83, no. 3, pp. 633–640, 2003.

[17] Y. Chen, A. Wiesel, Y. C. Eldar, and A. O. Hero, "Shrinkage algorithms for MMSE covariance estimation," *IEEE Trans. Signal Process.*, vol. 58, no. 10, pp. 5016–5029, 2010.

[18] A. Aubry, V. Carotenuto, A. De Maio, and G. Foglia, "Exploiting multiple a priori spectral models for adaptive radar detection," *IET Radar, Sonar & Navigation*, vol. 8, no. 7, pp. 695–707, August 2014.

[19] B. Kang, V. Monga, and M. Rangaswamy, "Rank-constrained maximum likelihood estimation of structured covariance matrices," *IEEE Trans. Aerosp. Electron. Syst.*, vol. 50, no. 1, pp. 501–515, January 2014.

[20] A. Aubry, A. De Maio, G. Foglia, and D. Orlando, "Diffuse multipath exploitation for adaptive radar detection," *IEEE Trans. Signal Process.*, vol. 63, no. 5, pp. 1268–1281, March 2015.